Edinburgh, Scotland
EURONOISE 2009
October 26-28

Broadband shock-associated noise predictions

Philip J. Morris [a]
Steven A. E. Miller [b]
The Pennsylvania State University
Department of Aerospace Engineering
University Park, Pa, 16802 USA

ABSTRACT

Broadband shock-associated noise (BBSAN) is generated when a jet operates off-design. This can occur in both military fighter aircraft turbojet engines and commercial turbofan engines, particularly at cruise conditions. The noise is generated by the interaction between the turbulence in the jet shear layer and the jet's shock cell structure. The present paper describes a model for BBSAN that uses steady RANS CFD to describe the jet flow and to provide information on the turbulence scales. The acoustic model is based on a rearrangement of the equations of motion into a propagation component (the linearized Euler equations) and a source component, which depends on products of the turbulent fluctuations and the shock cell pressure perturbations. A model is introduced to describe the statistical properties of the turbulence and the shock cell structure is determined from the RANS simulations. Predictions are made for circular and rectangular single stream jets, both unheated and heated, and both under- and over-expanded conditions. Comparisons of the predicted BBSAN spectra are made with experiments.

1. INTRODUCTION

Broadband shock-associated noise (BBSAN) is one component of jet noise from supersonic jets operating at off-design conditions. This component dominates the radiated noise at large angles relative to the jet downstream axis, when the jet is operating off-design. The method builds on the noise generation mechanisms that have been proposed in existing prediction methods, but the focus is on the development of a new BBSAN prediction scheme that is free of the limitations of previous models. Only the operating conditions of an off-design supersonic jet and the nozzle geometry need to be specified to make a prediction. The long term goal of the present approach is to make BBSAN predictions from nozzles that are not axisymmetric and include arbitrary off-design operating conditions. The results in the present paper are mostly for axisymmetric jets operating at a variety of nozzle pressure ratios *NPR* and total temperature ratios *TTR*. However, a calculation for a rectangular jet is also included.

Current prediction methods for BBSAN are based primarily on empirical correlations of radiated noise and jet flow data. These methods are restricted to axisymmetric single, dual-stream, or simple rectangular jet nozzle geometries. BBSAN is a very important component of noise in both unheated and heated jets. In heated jets, the BBSAN and mixing noise are often of similar intensity, though they radiate in different directions. Mixing noise is dominant in the jet's downstream arc and BBSAN is dominant in the upstream arc. However, this is only the case for the peak noise levels. At low frequencies in particular, the jet mixing noise is dominant at all angles to the jet axis. As will be shown, this is because the BBSAN spectrum decays very rapidly at low frequencies.

[a] Email address. pjm@psu.edu
[b] Email address. saem@psu.edu

Broadband shock-associated noise can occur for either convergent or convergent-divergent nozzles. An imbalance of pressure at the jet exit generates a system of shocks and expansions in the jet plume. The interaction between the turbulence in the jet shear layer and this shock cell structure is the source of shock-associated noise. Shock-associated noise is observed as a strong spectral peak, with multiple peaks of lower intensity at higher frequencies. It occurs at relatively large angles to the jet downstream axis. The peak frequency is a simple function of the jet shock cell spacing and the convection velocity of the jet shear layer turbulence. The amplitude of broadband shock-associated noise depends on the ratio of observer distance to the jet diameter, the polar and azimuthal observer angles, the jet diameter, the fully expanded jet velocity, and the degree of off-design operation.

The first prediction scheme for broadband shock-associated noise was developed by Harper-Bourne and Fisher[1]. Their proposition was that BBSAN depends on the nearly coherent interaction between the turbulence in the jet shear layer interacting with the jet's nearly periodic shock cell structure. This can be modeled as a series of correlated point sources that radiate either constructively or destructively. Harper-Bourne and Fisher's prediction scheme depends on a characteristic spectral shape of the radiated noise generated by each interaction. This was obtained using a least squares procedure to match the model with experimental noise measurements. A second prediction method for shock-associated noise was developed by Tam[2]. The basic physical model was that described by Tam and Tanna[3]. Tam[2] argued that the shock cell structure in the jet could be modeled, following the work of Pack[4], as modes in a waveguide, where the waves are forced by the pressure imbalance at the jet exit and are confined by the jet shear layer. The simplest model that can be used for the jet is a vortex sheet. The effects of the slow divergence of the jet and the dissipative effects of the turbulence on the shock cells can also be included in the same general framework, as shown by Tam, Jackson, and Seiner[5]. The large-scale turbulence in the jet shear is modeled as a random superposition of instability waves supported by the jet mean flow, as described by Tam and Chen[6]. The interaction between the downstream traveling instability waves and the nearly periodic shock cell structure results in an interference pattern of traveling waves. The phase velocity of these waves can be higher than that of the instability waves alone and gives rise to noise radiation at large angles to the jet downstream axis, including the upstream direction. Since there is a random set of instability waves interacting with the shock cells the resulting radiation pattern involves broad lobes rather than a sharply directional radiation. Tam argued that a complete calculation of the large scale turbulence spectrum would be computationally very expensive. So the eventual prediction formula is based on a simple growth and decay formula for the instability waves and their phase velocity and empirical formulas to correct the shock cell spacing from the vortex sheet solution. In addition, the spectral width is determined with a best fit to the measured noise data. The predictions give good agreement with noise measurements in both the jet's near and far fields and certain key features of the measured spectra are captured. These include the variation of the frequency of the broadband spectral peak with observation location (the same prediction is provided by the Harper-Bourne and Fisher[1] model), the presence of secondary spectral peaks at higher frequencies than the main peak, and their narrowing as the observer moves towards the jet upstream direction. Tam[7] extended his original model to account for jets operating at moderately off-design conditions as well as to incorporate a correction for the effect of jet heating (though no comparisons were shown for heated cases).

In the present approach, the development of the jet flow, including the internal flow in the nozzle, is predicted using a steady, Reynolds-averaged Navier Stokes (RANS) calculation. A two-equation turbulence model is used. These calculations are relatively fast in comparison to time-accurate flow simulations. The results of the RANS simulations are used to characterize the jet mean flow, including the jet's shock cell structure, as well as to provide estimates of the

turbulent fluctuation levels and the turbulent length and time scales. The incorporation of this information within the BBSAN noise model, described in the next section, enables the BBSAN to be predicted on the basis of the jet nozzle geometry and operating conditions alone.

2. BROADBAND SHOCK ASSOCIATED-NOISE MODEL DEVELOPMENT

The BBSAN model builds on the analysis developed by Tam[2]. Tam's analysis is considerably simplified if the following form of the inviscid compressible equations of motion is used.

$$\frac{D\pi}{Dt}+\frac{\partial v_i}{\partial x_i}=0, \tag{1}$$

$$\frac{Dv_i}{Dt}+a^2\frac{\partial \pi}{\partial x_i}=0, \tag{2}$$

where,

$$\frac{D}{Dt}=\frac{\partial}{\partial t}+v_i\frac{\partial}{\partial x_i}. \tag{3}$$

a is the local speed of sound, t is time, and v_i are the velocity components in the x_i directions of a Cartesian coordinate system. π is defined by, $\pi=(1/\gamma)\ln\left(p/p_\infty\right)$, where p is the pressure, p_∞ is the ambient pressure, and γ is the ratio of specific heats of an ideal gas. Following Tam[2], the instantaneous flow-field properties are separated into four components. That is,

$$\begin{pmatrix}\pi\\ v_i\end{pmatrix}=\begin{pmatrix}\overline{\pi}+\pi_s+\pi_t+\pi'\\ \overline{v}_i+v_{si}+v_{ti}+v_i'\end{pmatrix}, \tag{4}$$

where the overbar denotes the long time averaged value, the subscript s denotes the perturbations associated with the shock cell structure, the subscript t denotes the fluctuations associated with the turbulence, and the primes denote the fluctuations generated by the interaction of the turbulence and the shock cell structure. It will be assumed that the shock cell structure satisfies the steady linearized version of Eqns. (1) and (2). In addition, it is assumed that the unsteady linearized version of these equations is also satisfied by the turbulent velocity fluctuations. This is justified if the important components of the turbulence, so far as the broadband shock-associated noise is concerned, are coherent over relatively large axial distances. These components are described well by a linear instability wave model. If disturbances of this form are substituted into the full equations, subject to the preceding assumptions, then the equations for the BBSAN fluctuations are found to be,

$$\frac{\partial \pi'}{\partial t}+\overline{v}_j\frac{\partial \pi'}{\partial x_j}+\frac{\partial v_i'}{\partial x_i}=\theta \tag{5}$$

$$\frac{\partial v_i'}{\partial t}+\overline{v}_j\frac{\partial v_i'}{\partial x_j}+v_j'\frac{\partial \overline{v}_i}{\partial x_j}+\overline{a}^2\frac{\partial \pi'}{\partial x_i}=f_i^v+f_i^a \tag{6}$$

The primary source term considered here, if the effects of fluctuations in the speed of sound are ignored, can be written,

$$f_i^v=-v_{sj}\frac{\partial v_{ti}}{\partial x_j}-v_{tj}\frac{\partial v_{si}}{\partial x_j}, \tag{7}$$

where f_i^v is the unsteady force per unit volume associated with interactions between the turbulent velocity fluctuations and the velocity perturbations associated with the shock cells. The solution to Eqns. (5) and (6), can be written in terms of the vector periodic Green's functions,

$\pi_g{}^n(\mathbf{x},\mathbf{y},\omega)$, where ω is the radian frequency. Also, for small perturbation pressures, $\pi' \sim p'/\gamma p_\infty = p'/\rho_\infty a_\infty{}^2$. Then the solution for the far-field pressure $p'(\mathbf{x},t)$ can be written,

$$p'(\mathbf{x},t) = \rho_\infty a_\infty^2 \int_{-\infty}^{\infty}\int_{-\infty}^{\infty}\sum_{n=1}^{3} \pi_g^n(\mathbf{x},\mathbf{y},t-\tau) f_n^v(\mathbf{y},\tau) \Big\} d\tau d\mathbf{y}. \tag{8}$$

Now the autocorrelation of the pressure can be formed and the spectral density is given by the Fourier transform of the autocorrelation of the pressure. The autocorrelation for the pressure depends on the two point cross correlation of f_n^v. In turn, this is dependent on the strength of the shock cells and the turbulent velocity fluctuations whose product is significant in regions where the shocks and expansions intersect with the turbulent shear layer. It is assumed that the two-point cross correlation function of the BBSAN source term can be written as,

$$\overline{f_n^v(\mathbf{y},\tau_1) f_m^v(\mathbf{z},\tau_2)} = R_{nm}^v(\mathbf{y},\boldsymbol{\eta},\tau), \tag{9}$$

where, $\boldsymbol{\eta} = \mathbf{z} - \mathbf{y}$ and $\tau = \tau_2 - \tau_1$. This is consistent with the statistics of the turbulence being locally a function of the separation distance and time delay between the two source locations. Then, following some straightforward integrations, the spectral density for the pressure can be written as,

$$S(\mathbf{x},\omega) = \rho_\infty^2 a_\infty^4 \int_{-\infty}^{\infty}\cdots\int_{-\infty}^{\infty}\sum_{n=1}^{3}\sum_{m=1}^{3} \pi_g^n(\mathbf{x},\mathbf{y},-\omega)\pi_g^m(\mathbf{x},\mathbf{y}+\boldsymbol{\eta},\omega) R_{nm}^v(\mathbf{y},\boldsymbol{\eta},\tau)\exp(i\omega\tau)\, d\tau d\boldsymbol{\eta} d\mathbf{y} \tag{10}$$

The Green's functions could be calculated numerically for a given mean flow. This could involve a locally parallel approximation or the full diverging flow. Also, the problem could be formulated in terms of the adjoint Green's function for the linearized Euler equations as described by Tam and Auriault[8]. However, BBSAN is radiated predominantly at large angles to the jet downstream axis where the refractive effects of the mean flow would be small or absent. In view of this, the Green's function is approximated by the Green's function in the absence of a mean flow. The components of the vector Green's function are then readily related to the Green's function of the Helmholtz equation. With the use of these approximate forms for the far field Green's functions, the spectral density can be written as,

$$S(\mathbf{x},\omega) = \frac{\rho_\infty^2\omega^2}{16\pi^2 a_\infty^2 x^2}\int_{-\infty}^{\infty}\cdots\int_{-\infty}^{\infty}\frac{x_n x_m}{x^2} R_{nm}^v(\mathbf{y},\boldsymbol{\eta},\tau)\exp\left[i\omega\left(\tau - \frac{\mathbf{x}\cdot\boldsymbol{\eta}}{x a_\infty}\right)\right] d\tau d\boldsymbol{\eta} d\mathbf{y}. \tag{11}$$

The summation terms in Eqn. (11) are not shown but are implied by the repeated subscripts n and m. From the form of f_i^v given by Eqn. (7), and on dimensional grounds, it is taken to scale as,

$$f_i^v \sim \frac{p_s v_t}{\rho_\infty a_\infty l}, \tag{12}$$

where p_s represents the shock cell pressure, v_t is a characteristic turbulent velocity fluctuation, and l is a characteristic turbulent length scale. These will be determined from the RANS CFD solution. Also, for simplicity, use is made of the Proudman form for the cross correlation. This represents an isotropic assumption for the turbulent velocity statistics. Use of these relationships gives,

$$R_{xx}^v(\mathbf{y},\boldsymbol{\eta},\tau) = \frac{1}{\rho_\infty^2 a_\infty^2 l^2} p_s(\mathbf{y}) p_s(\mathbf{y}+\mathbf{h}) R^v(\mathbf{y},\boldsymbol{\eta},\tau), \tag{13}$$

where,

$$R^v(\mathbf{y},\boldsymbol{\eta},\tau) = \overline{v_x(\mathbf{y},t) v_x(\mathbf{y}+\boldsymbol{\eta},t+\tau)} \tag{14}$$

is the two-point cross correlation function of the turbulent velocity fluctuations in the observer direction. The far field spectral density can then be written as,

$$S(\mathbf{x},\omega)=\frac{\omega^2}{16\pi^2 a_\infty^4 x^2}\int_{-\infty}^{\infty}\cdots\int_{-\infty}^{\infty}\frac{1}{l^2}\,p_s(\mathbf{y})\,p_s(\mathbf{y}+\boldsymbol{\eta})\,R^v(\mathbf{y},\boldsymbol{\eta},\tau)\exp\left[i\omega\left(\tau-\frac{\mathbf{x}\cdot\boldsymbol{\eta}}{xa_\infty}\right)\right]d\tau d\boldsymbol{\eta}d\mathbf{y}. \tag{15}$$

In order to emphasize the quasi-periodic nature of the shock cell structure and to assist in the implementation of the model, the axial spatial Fourier transform of the shock cell's pressure perturbation is defined. The axial Fourier transform of the shock cell pressure is given by,

$$\tilde{p}_s(k_1,y_2,y_3)=\int_{-\infty}^{\infty}\tilde{p}_s(\mathbf{y})\exp[-ik_1y_1]dy_1. \tag{16}$$

The axial Fourier transform of the shock pressure can be substituted into Eqn. (15). It should be noted that this transform of the shock cell pressure perturbation is only applied to one of the two terms in the integrand. This has been found to be convenient in the evaluation of the BBSAN noise prediction formula given below.

A model is now proposed for $R^v(\mathbf{y},\boldsymbol{\eta},\tau)$ in the form,

$$R^v(\mathbf{y},\boldsymbol{\eta},\tau)=K\exp\left[-|\tau|/\tau_s\right]\exp\left[-\left(\xi-\bar{u}_c\tau\right)^2/l^2\right]\exp\left[-\left(\eta^2+\zeta^2\right)^2/l_\perp^2\right]. \tag{17}$$

τ_s is the turbulent time scale, $l_\perp$ is the turbulent length scale in the cross-stream direction, and K is the turbulent kinetic energy. The scales, τ_s, l, and $l_\perp$ are found directly from the CFD RANS solution. The observer location is now written in spherical polar coordinates, $\mathbf{x}=x(\sin\theta\cos\varphi,\sin\theta\sin\varphi,\cos\theta)$. Then, after some integrations and simplifications, the far field spectral density can be written as,

$$\begin{aligned}S(\mathbf{x},\omega)=\frac{1}{\pi\sqrt{\pi}a_\infty^4x^2}\int_{-\infty}^{\infty}\cdots\int_{-\infty}^{\infty}\Bigg\{&\frac{Kl_\perp^2}{l\tau_s}\,p_s(\mathbf{y})\,\tilde{p}_s(k_1,y_2,y_3)\exp(ik_1y_1)\\&\times\frac{\omega^2\tau_s^2\left\{\exp\left[-l^2\left(k_1-\omega\cos\theta/a_\infty\right)^2/4-\omega^2l_\perp^2\sin^2\theta/4a_\infty^2\right]\right\}}{\left[1+\left(1-M_c\cos\theta+\bar{u}_ck_1/\omega\right)^2\omega^2\tau_s^2\right]}\Bigg\}dk_1d\mathbf{y}\end{aligned} \tag{18}$$

Equation (18) provides the prediction formula for the BBSAN. All of the parameters can be determined from a RANS CFD solution. In the case of an axisymmetric jet the integrations with respect to the cross stream direction can be reduced to a single integration in the radial direction.

3. IMPLEMENTATION

The implementation of the BBSAN model developed in the previous section requires a RANS solution from a CFD solver using a two equation turbulence model. The NPARC alliance Wind-US[9] CFD solver is used to generate the RANS solutions. The RANS solutions found with Wind-US use the Menter[10] SST turbulence model that provides the mean quantities, including *K* and *Ω*, where *K* is the turbulent kinetic energy per unit volume and *Ω* is the specific dissipation rate. The viscous dissipation rate is given by $\varepsilon=0.09\Omega K$. The number of grid points in a typical calculation is 200,000 to 500,000. Solutions of the flow-field are over-resolved and a much lower number of grid points in the computational domain could be used. The flows have been over-resolved so grid independence studies of the various BBSAN calculations could be performed by interpolating to lower resolutions.

To validate the axisymmetric RANS solutions for off-design supersonic jets, two sets of CFD simulations have been compared with experimental results. These include a convergent nozzle, with design Mach number, $M_d=1.0$, and a convergent-divergent nozzle, $M_d=1.5$. The

convergent nozzle operates at an *NPR* = 3.671 and the convergent-divergent nozzle operates at an *NPR* = 2.771. Both RANS solutions are for unheated jets with a *TTR* = 1.0. The geometry of both nozzles is the same as those used in experiments performed at Penn State University (PSU). Mach number, total pressure, and static pressure measurements have been compared with the same quantities from the Wind-US solutions at various downstream locations. Additionally, schlieren comparisons have been made to compare the relative positions of the shocks and expansions in the jet. Results for the convergent-divergent jet have also shown excellent agreement. Full details of the CFD validation for axisymmetric jets are given by Miller *et al.*[11].

The characteristic scales required in the BBSAN model are found from *K* and *ε* from the RANS solutions. The time and length scales are taken to be, $\tau_s = c_\tau K/\varepsilon$, $l = K^{3/2}/\varepsilon$, and $l_\perp = c_\perp l$, where c_τ, c_l, and $c_\perp$ are coefficients. An additional factor, P_f, is needed in the model to scale the amplitude of the spectral density. The scaling is the same for all jet operating conditions and a good value is $P_f = 10^{3/2} \equiv +15dB$. The constants used in all the predictions shown below are $c_\tau = 1.25$, $c_l = 3.25$, and $c_\perp = 0.3$. These constants have been found by performing a parametric study relative to a single selected jet condition and observer angle with various sets of experimental data.

3. RESULTS

BBSAN predictions have been made for the jets based on the Wind-US CFD solutions using the Menter SST turbulence model. The cases selected include both unheated and heated jets operating at over-$\left(M_j < M_d\right)$ and under-expanded $\left(M_j > M_d\right)$ conditions for two different nozzle geometries with design Mach numbers, $M_d = 1.0$ and $M_d = 1.5$. M_j is the fully-expanded Mach number. The CFD simulations for all the cases use a jet exit diameter, $D = 0.0127$ m. However, other CFD simulations for the same operating conditions but with different diameters have been performed and results are similar for the BBSAN.

The BBSAN predictions are made at various angles θ from the downstream jet axis at a radial polar distance of 100 diameters (D) from the center of the jet exit. Predictions are lossless and humidity and atmospheric absorption corrections have been applied to the corresponding experimental data in each case so that the measured SPL are also lossless. The experimental data provided by Boeing was measured at 97.5 D from the nozzle exit while the Pennsylvania State University (PSU) data was measured at 150 D. Both sets of data have been corrected to 100 D. The Boeing experiments were performed with heated air while the PSU experiments were performed with Helium/Air mixtures to simulate heated jets. The diameter of the convergent nozzle in the Boeing experiments was 0.0622 m (2.45 in.) while the diameter of the PSU nozzle was 0.0127 m (1/2 in.). Experimental data, measured in the Small Hot Jet Aeroacoustic Research (SHJAR) facility at NASA Glenn Research Center, have also been used for evaluation of the predictions. The SHJAR jet is a 0.0508 m (2 in.) diameter nozzle with microphones at a polar distance of 50 diameters.

The model developed in the present paper is only for the BBSAN, which is only one of the components of off-design supersonic jet noise. Thus, it is useful to separate the individual noise components from the total spectrum. Viswanathan[12] has developed a framework that separates the individual components of the total noise spectra into mixing noise and BBSAN. The Boeing

data presented below for the converging nozzle predictions show this breakdown to help illustrate the capability of the prediction scheme.

The case that has been used to determine the coefficients for the turbulence scales is an under-expanded converging jet with $M_j = 1.5$ and *TTR* = 1.00. Results of the model prediction in this case, in addition to various experiments, are shown in Figure 1. There are eight comparisons of the predictions with experimental data for different observer angles θ with respect to the downstream jet axis. Each comparison is labeled with its corresponding observer angle and the maximum SPL level of the experiments from Boeing. The screech tones are not used to find the maximum value. It could be argued that the choice of a case with screech is not the best choice, and that will be corrected in the future. Experimental data from Boeing, NASA, and PSU are shown for each observer angle. Though there are minor differences between the different sets of experimental data, the overall agreement is good. Also shown are predictions based on the BBSAN prediction formulas provided by Tam[2] or Tam[7] where appropriate. The breakdown of the total Boeing spectra into the BBSAN and mixing noise components is also shown. The predictions capture the multiple peaks in the BBSAN spectra as well as the broadening in the spectral shape with decreasing angle to the jet downstream axis. It is important to emphasize that the predictions at every angle use the same scaling coefficients. The increase in the relative importance of the mixing noise at lower Strouhal numbers is evident in the experiments.

The wavenumber integration in Eqn. (18) can be limited to contributions associated with individual components of the shock cell's wavenumber spectrum. This is equivalent to examining the contributions of the interactions of the turbulence with the Fourier modes in a waveguide model of the shock cell structure. Figure 2 shows these contributions and the corresponding peaks that they generate in the BBSAN spectrum. This selection of wavenumber ranges replaces the summation over Fourier components of the waveguide model for the shock cell structure in Tam's model[2]. However, in the present model, the spectral width is controlled by both the spectrum shape associated with the turbulent velocity fluctuations and the finite bandwidth of the dominant lines in the Fourier transform representation of the shock cell structure.

An over-expanded prediction for $M_d = 1.5$, $M_j = 1.3$, and *TTR* = 2.20 is shown in Figure 3. In this heated case, there is good agreement between the predictions and the experiments. There is also close agreement between the present predictions and Tam's model[7] in this heated case. The developed BBSAN model better predicts the BBSAN between each broad peak unlike the model of Tam. The peak BBSAN predictions agree relatively well between the two prediction methods and are only 1 to 2 dB different to the experimental peak amplitude.

The final prediction shown is for a rectangular nozzle in the major axis plane at 100 degrees to the downstream axis. The rectangular jet has an aspect ratio of 1.75 of the exit height to exit width. The BBSAN spectrum is shown in Figure 4 and is compared with data obtained at PSU. Very little variation in the experimental results occurs in the azimuthal direction for rectangular jets with such a low aspect ratio. The maximum variation is observed to be only 1 or 2 dB. The primary BBSAN peak and the peaks at higher frequencies are captured and the corresponding peaks can be seen in the BBSAN spectrum. Although, the predicted BBSAN at high frequencies has a fall-off that is too high. This could easily be corrected by lowering c_τ or $c_\perp$.

4. CONCLUSIONS

A model for Broadband Shock-Associated Noise in supersonic jets operating at off-design conditions has been developed and implemented. It attempts to overcome the limitations of

previous models by reducing empiricism and by basing the predictions on RANS CFD flow field calculations. Only the geometry of the nozzle and its operating conditions need to be known to construct the RANS solution and the associated BBSAN predictions. The model has been calibrated by adjusting the scaling coefficients that represent the relevant turbulent length and times scales at one operating condition only. Overall, the predicted spectral densities for off-design supersonic jets agree well with experimental data. In order to provide a consistent assessment of the prediction method, the amplitude scaling has been fixed for all operating conditions.

ACKNOWLEDGMENTS

This research is sponsored by a NASA Cooperative Agreement NNX07AC88A entitled, “A Comprehensive Model for the Prediction of Supersonic Jet Noise.” The Technical Monitor for the Cooperative Agreement is Dr. Milo Dahl of the NASA Glenn Research Center. The authors are grateful for the experimental data provided by Drs. Jeremy Veltin, Dennis K. McLaughlin, and Mr. Ching-Wen Kuo of The Pennsylvania State University, Dr. K. Viswanathan of the Boeing Company, and Dr. James Bridges of the NASA Glenn Research Center.

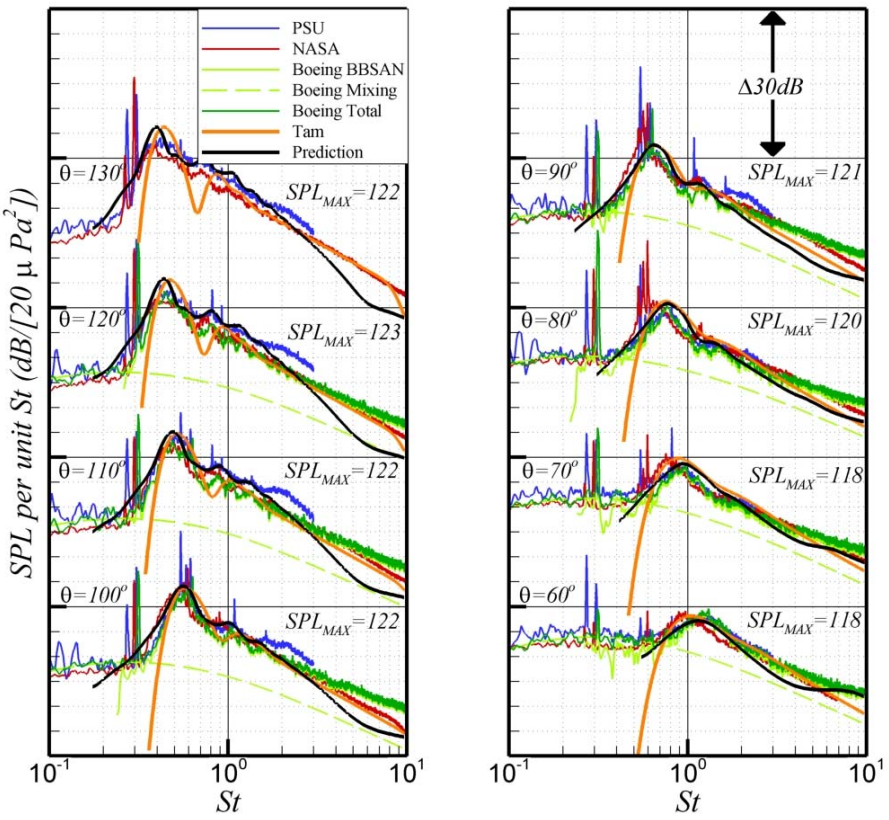

Figure 1: Comparisons of BBSAN predictions with experiments for $M_d = 1.0,\ M_j = 1.5$, *TTR* = 1.00, $R/D = 100$.

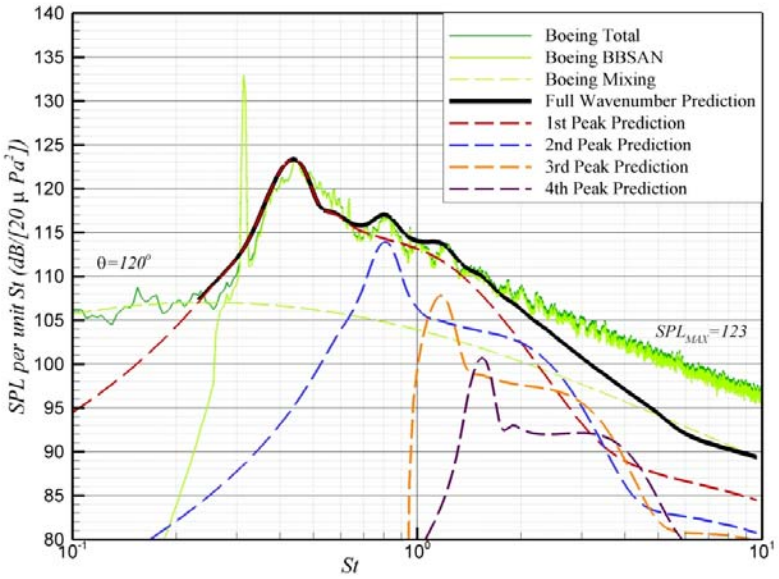

Figure 2: The total BBSAN prediction and the accompanying contributions from selective integrations over contributing wavenumbers of ~p_s representing different waveguide modes of the shock cell structure. $M_d = 1.0,\ M_j = 1.5$, *TTR* = 1.00, $R/D = 100,\ \theta = 120^o$.

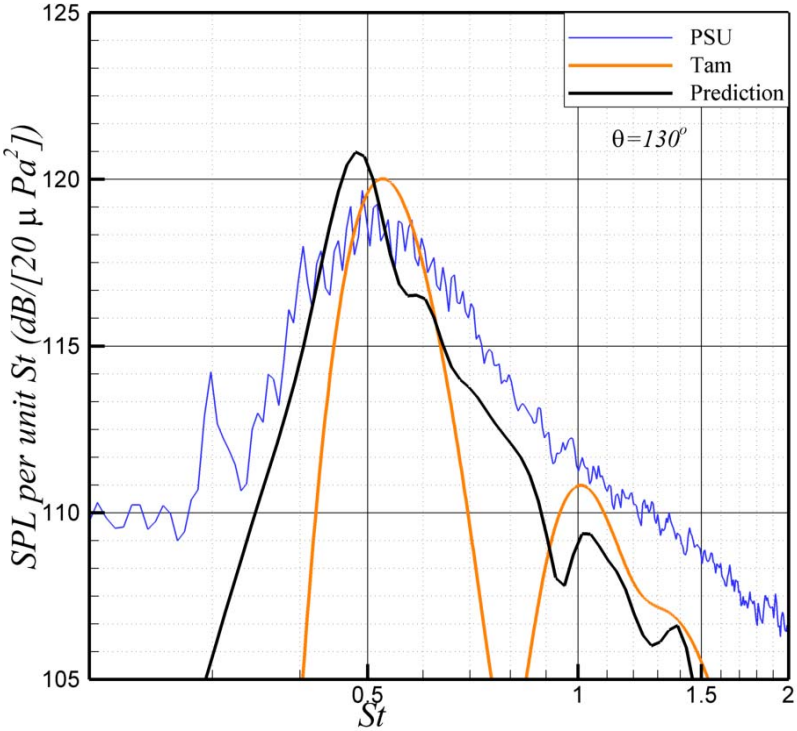

Figure 3: Comparisons of BBSAN predictions with experiments for $M_d = 1.5,\ M_j = 1.3$, *TTR* = 2.20, $R/D = 100,\ \theta = 130^o$.

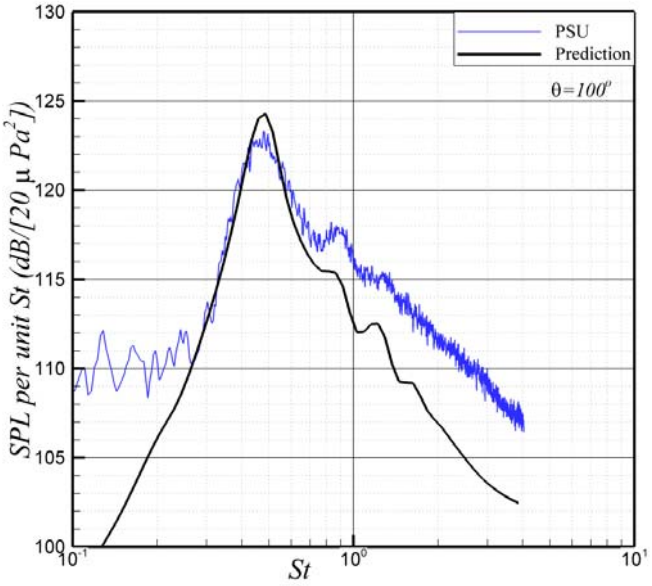

Figure 4: Comparisons of BBSAN predictions with experiments for, $M_d = 1.5,\ M_j = 1.7$, *TTR* = 1.00, $R/D = 100,\ \theta = 100^o$ in the major axis plane.

REFERENCES

1. M. Harper-Bourne and M. J. Fisher, "The noise from shock waves in supersonic jets", in Proceedings (No. 131) of the AGARD Conference on Noise Mechanisms, Brussels, Belgium, 1973.
2. C. K. W. Tam, Stochastic model theory of broadband shock associated noise from supersonic jets, *Journal of Sound and Vibration*, **116**(2), pp. 265-302, (1987).
3. C. K. W. Tam and H. K. Tanna, Shock-associated noise of supersonic jets from convergent-divergent nozzles, *Journal of Sound and Vibration*, **81**(3), pp. 337-358 (1982).
4. D. C. Pack, A note on Prandtl's formula for the wavelength of a supersonic gas jet, *Quarterly Journal of Applied Mathematics and Mechanics*, **3**, pp. 173-181, (1950).
5. C. K. W. Tam, J. A. Jackson, and J. M. Seiner, A multiple-scales model of the shock-cell structure of imperfectly expanded supersonic jets, *Journal of Fluid Mechanics*, **153**, pp. 123-149, (1985).
6. C. K. W. Tam and K. C. Chen, A statistical model of turbulence in two-dimensional mixing layers, *Journal of Fluid Mechanics*, **92**, pp. 303-326, (1979).
7. C. K. W. Tam, Broadband shock-associated noise of moderately imperfectly-expanded supersonic jets, *Journal of Sound and Vibration*, **140**(1), pp. 55-71, (1990).
8. C. K. W. Tam and L. Auriault, Mean flow refraction effects on sound radiated from localized sources in a jet, *Journal of Fluid Mechanics*, **370**, pp. 149-174, (1998).
9. C. Nelson and G. Power, "The NPARC Alliance flow simulation system", AIAA Paper 2001-0594, 2001.
10. F. R. Menter, Two-equation eddy-viscosity turbulence models for engineering applications, *AIAA Journal*, **32**(8), pp. 1598-1605, (1994).
11. S. A. E. Miller, J. Veltin, P. J. Morris, and D. K. McLaughlin "Validation of computational fluid dynamics for supersonic shock containing jets", AIAA Paper 2008-2988, 2008.
12. K. Viswanathan, Scaling laws and a method for identifying components of jet noise, *AIAA Journal*, **44**(10), pp. 2274-2285, (2006).